Monthly Notices
of the
ROYAL ASTRONOMICAL SOCIETY

MNRAS **475,** 469–477 (2018)
Advance Access publication 2017 December 7

doi:10.1093/mnras/stx3157

PSR J2322−2650 – a low-luminosity millisecond pulsar with a planetary-mass companion

R. Spiewak,[1⋆] M. Bailes,[1,2] E. D. Barr,[3] N. D. R. Bhat,[4] M. Burgay,[5] A. D. Cameron,[3] D. J. Champion,[3] C. M. L. Flynn,[1] A. Jameson,[1,6] S. Johnston,[7] M. J. Keith,[8] M. Kramer,[3,8] S. R. Kulkarni,[9] L. Levin,[8] A. G. Lyne,[8] V. Morello,[8] C. Ng,[10] A. Possenti,[5] V. Ravi,[9] B. W. Stappers,[8] W. van Straten[11] and C. Tiburzi[3,12]

[1]*Centre for Astrophysics and Supercomputing, Swinburne University of Technology, PO Box 218, Hawthorn, VIC 3122, Australia*
[2]*ARC Centre of Excellence for Gravitational Wave Discovery (OzGrav), Mail H29, Swinburne University of Technology, PO Box 218, Hawthorn, VIC 3122, Australia*
[3]*Max-Planck-Institut für Radioastronomie, Auf dem Hügel 69, D-53121 Bonn, Germany*
[4]*International Centre for Radio Astronomy Research, Curtin University, Bentley, WA 6102, Australia*
[5]*INAF – Osservatorio Astronomico di Cagliari, via della Scienza 5, I-09047 Selargius, Italy*
[6]*ARC Centre of Excellence for All-Sky Astronomy (CAASTRO), Mail H30, Swinburne University of Technology, PO Box 218, Hawthorn, VIC 3122, Australia*
[7]*CSIRO Astronomy and Space Science, Australia Telescope National Facility, PO Box 76, Epping, NSW 1710, Australia*
[8]*Jodrell Bank Centre for Astrophysics, University of Manchester, Alan Turing Building, Oxford Road, Manchester M13 9PL, UK*
[9]*Cahill Center for Astronomy and Astrophysics, MC 249-17, California Institute of Technology, Pasadena, CA 91125, USA*
[10]*Department of Physics and Astronomy, University of British Columbia, 6224 Agriculture Road, Vancouver, BC V6T 1Z1, Canada*
[11]*Institute for Radio Astronomy and Space Research, Auckland University of Technology, Private Bag 92006, Auckland 1142, New Zealand*
[12]*Fakultät für Physik, Universität Bielefeld, Postfach 100131, D-33501 Bielefeld, Germany*

Accepted 2017 November 30. Received 2017 November 21; in original form 2017 August 10

ABSTRACT

We present the discovery of a binary millisecond pulsar (MSP), PSR J2322−2650, found in the southern section of the High Time Resolution Universe survey. This system contains a 3.5-ms pulsar with a $\sim 10^{-3}$ $M_\odot$ companion in a 7.75-h circular orbit. Follow-up observations at the Parkes and Lovell telescopes have led to precise measurements of the astrometric and spin parameters, including the period derivative, timing parallax, and proper motion. PSR J2322−2650 has a parallax of 4.4 ± 1.2 mas, and is thus at an inferred distance of 230^{+90}_{-50} pc, making this system a candidate for optical studies. We have detected a source of $R \approx 26.4$ mag at the radio position in a single R-band observation with the Keck telescope, and this is consistent with the blackbody temperature we would expect from the companion if it fills its Roche lobe. The intrinsic period derivative of PSR J2322−2650 is among the lowest known, $4.4(4) \times 10^{-22}$ s s^{-1}, implying a low surface magnetic field strength, $4.0(4) \times 10^7$ G. Its mean radio flux density of 160 μJy combined with the distance implies that its radio luminosity is the lowest ever measured, 0.008(5) mJy kpc^2. The inferred population of these systems in the Galaxy may be very significant, suggesting that this is a common MSP evolutionary path.

Key words: pulsars: general – pulsars: individual: PSR J2322−2650.

1 INTRODUCTION

Since the discovery of pulsars (Hewish et al. 1968), more than 2500 have been detected with a wide range of spin periods and magnetic field strengths. The majority of known pulsars are isolated, but roughly 10 per cent have companions with masses ranging from $\sim 10^{-6}$ to $\sim 10^{1}$ $M_\odot$.

At irregular intervals, new types of pulsars are discovered that lead to breakthroughs in our understanding of theories of relativistic gravity or the pulsar emission mechanism, or how pulsars evolve. For example, the discovery of the double pulsar led to new tests of general relativity (Burgay et al. 2003; Lyne et al. 2004), and the discovery of intermittent pulsars demonstrated that a radio pulsar's emission mechanism could exhibit bimodal behaviour (Kramer et al. 2006).

After the discovery of the first binary pulsar, PSR B1913+16 (Hulse & Taylor 1975), also known as the Hulse–Taylor pulsar, Bisnovatyi-Kogan & Komberg (1976) described a possible course

⋆ E-mail: renee.spiewak@gmail.com

Table 1. Follow-up observations of J2322−2650 – receiver information.

Telescope	Receiver	Backend	Centre frequency (MHz)	Recorded BW (MHz)	Obs. used/recorded	Dates (MJD)
Lovell		ROACH	1520	512	239/279	56129–57848
Parkes	MB	CASPSR	1382	400	30/44	56174–57261, 57761–57870
		DFB3[a]	1369	256	2/23	56156–56739
		DFB4[a]			2/21	56953–57341, 57761–57823
	H-OH	CASPSR	1400	400	8/9	57472–57703
		DFB4[a]	1369	256	0/7	57621–57703
	10/50 cm	CASPSR	728	200	0/2	56511, 57846
		DFB3	732	64	0/2	56504, 56511
		DFB4	3100	1024	2/3	56504, 56511, 57846

Note. [a]CASPSR observations preferentially used where overlapping with DFB data in the same band.

of evolution of the system through an X-ray bright phase, during which the magnetic field of the pulsar is weakened and the pulsar's spin period reduced. When the first millisecond pulsar (MSP) was discovered by Backer et al. (1982), Alpar et al. (1982) proposed an evolutionary track for ordinary pulsars to be spun up to millisecond periods by mass transferred from a binary companion, listing low-mass X-ray binaries (LMXBs) among the possible progenitors. In the intervening 35 yr, this has become the standard model for MSP production (see e.g. Deloye 2008), and some systems have been observed to transition between the LMXB and radio MSP states (e.g. PSR J1227−4853; Roy et al. 2015), providing support for the model proposed by Alpar et al. (1982). In this model, the mass of a neutron star's companion largely determines the final spin period of the recycled pulsar. Low-mass companions lead to MSPs [isolated or with white dwarf (WD) companions], whereas higher mass stars may themselves create a neutron star, leading to a system resembling the Hulse–Taylor pulsar.

The discovery of planets orbiting a pulsar (PSR B1257+12; Wolszczan & Frail 1992) challenged theorists to explain the formation of such systems, as did the discovery of the 'diamond planet' pulsar (PSR J1719−1438; Bailes et al. 2011). In fact, of the 2613 pulsars in the Australia Telescope National Facility (ATNF) Pulsar Catalogue (v.1.56; Manchester et al. 2005), only four in the field have planetary-mass companions (defined as having masses less than $10^{-2}\,M_{\odot}$): PSRs J0636+5128[1] (Stovall et al. 2014), B1257+12, J1311−3430 (Pletsch et al. 2012), and J1719−1438. These pulsars are all MSPs, around which it is comparatively easy to detect low-mass companions via pulsar timing (see Wolszczan 1997), whereas no such low-mass companions have been detected around young pulsars (Kerr et al. 2015). Various hypotheses have been proposed for the formation of the above systems, ranging from near-complete ablation of a companion, to the inheritance of planets formed around a main-sequence star before the formation of the pulsar, to the development of planets in supernova fallback discs around young pulsars. These models and their implications have been discussed in several papers (e.g. Miller & Hamilton 2001; Wang, Kaplan & Chakrabarty 2007; Martin, Livio & Palaniswamy 2016). Discoveries of new pulsars with planetary-mass companions are needed to expand our knowledge of the evolutionary scenarios and to discriminate among them.

The High Time Resolution Universe (HTRU) pulsar survey is a highly successful pulsar survey, which uses the multibeam receiver on the Parkes telescope (Staveley-Smith et al. 1996) to observe the southern sky (Keith et al. 2010), with the northern sky covered by the Effelsberg 100-m Radio Telescope in Germany (Barr et al. 2013). To date, 996 pulsars have been detected in the southern part of HTRU, of which 171 are new discoveries, according to the ATNF Pulsar Catalogue.

In this work, we define an MSP as a pulsar with rotational period less than 20 ms and spin-down rate less than $10^{-17}\,s\,s^{-1}$. When deriving companion masses, if the pulsar mass is not known, we adopt the standard value of $1.4\,M_{\odot}$. The layout of the paper is as follows. In Section 2, we give an overview of the discovery of PSR J2322−2650, and describe follow-up timing and optical observations. In Section 3, we describe the system parameters found through timing and compare this with properties of other known pulsars. In Section 4, we look at how the system compares with other pulsars with planetary-mass companions and postulate possible formation scenarios for this system, and, finally, we offer some general conclusions in Section 5.

2 TIMING OBSERVATIONS

2.1 Discovery of PSR J2322−2650

PSR J2322−2650 was discovered in the HTRU high-latitude survey with Parkes on 2011 May 4 in a 285-s observation at 1400 MHz. The initial detection had a signal-to-noise ratio (S/N) of ≈12, and the source was confirmed with observations (starting 2012 July) with the Lovell Telescope at the Jodrell Bank Observatory (JBO) at a centre frequency of 1520 MHz. At the time of the initial detection, the flux density was ≈0.27 mJy (from the radiometer equation and taking into account the offset from boresight). The pulsar had a period of 3.463 ms and a dispersion measure (DM) of 6.18 pc cm^{-3} in the discovery observation. Follow-up observations soon revealed an orbit with a period of 7.75 h and projected semimajor axis of only 0.0028 lt-s.

2.2 Timing programs

Follow-up timing of J2322−2650 was carried out using the Parkes and Lovell telescopes, as described in Table 1. The timing data from Parkes (project ID P789) span a period of 4.8 yr, from MJD 56174 to 57846, with multiple receivers and pulsar processing systems. The majority of the observations at Parkes use the multibeam (MB) receiver, which has a frequency range of 1220–1520 MHz and cold-sky system equivalent flux density of 29 Jy (for the centre

[1] Originally, PSR J0636+5128 was published by Stovall et al. (2014) as PSR J0636+5129, but the designation has been corrected by Arzoumanian et al. (in preparation).

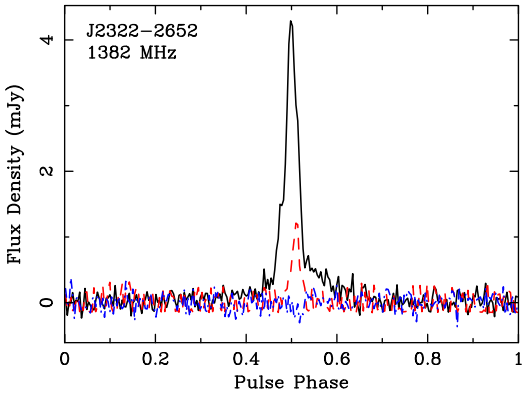

Figure 1. Integrated pulse profile from summed observations (equivalent integration time ∼50 ks) with linear (red dashed line) and circular (blue dash–dotted line) polarizations. The profile is well approximated by a small number of Gaussian components and has an FWHM of 3 per cent.

beam).[2] We used the H–OH receiver when the MB system was not available (2016 March 25–November 11), and the 10/50 cm receiver for greater spectral coverage. The backends used are the ATNF digital filterbanks (DFBs) and CASPSR.[3] The CASPSR backend coherently dedisperses the data, whereas the DFB backends do not, although, for a pulsar with such a small DM, this makes little practical difference. Observations with the Lovell Telescope cover the MJD range 56129–57848 and make use of a cryogenically cooled dual-polarization receiver with optimal performance in the frequency range 1350–1700 MHz. The cold-sky system equivalent flux density of the system is 25 Jy. The ROACH-based backend[4] Nyquist samples the 512-MHz-wide band at 8-bit resolution and divides the band into 32 × 16 MHz wide subbands (Bassa et al. 2016). Each subband is coherently dedispersed and folded in real time with the resultant pulse profiles stored with 1024 bins across the pulse profile. The subbands are combined in offline processing and, with the removal of known radio frequency interference (RFI) signals, a total bandwidth (BW) of approximately 384 MHz is used.

Data from the Parkes observations were calibrated for flux and polarization information using separate observations of Hydra A from the Parkes P456 project. The data from the Lovell Telescope are not flux- or polarization calibrated, but these effects are negligible for timing purposes, given the low polarization fraction. Fig. 1 shows the integrated profile from the sum of several observations (to an equivalent integration time of ∼50 ks) performed using the MB system and the CASPSR backend. At 1400 MHz, the mean flux density is $S_{1400} = 0.16(2)$ mJy (with the mean measurement uncertainty). The low S/N of the observations and significant instrumental effects make determination of the rotation measure difficult, even with the summed observations. Similarly, accurate measurement of the polarization position angle across the pulse is not possible. However, as the pulse profile is narrow [full width at half-maximum (FWHM) = 0.11(1) ms at 1400 MHz], precision timing is still possible. Because of interstellar scintillation, only ∼5 per cent of the flux-calibrated timing observations have flux density $S_{1400} \gtrsim 0.27$ mJy, the flux density at the time of discovery. J2322−2650 was not detected in four observations at 700 MHz with the Parkes 10/50 cm receiver, implying a flux density of $S_{700} \lesssim 0.1$ mJy for those epochs. In observations at 3100 MHz, the pulsar was detected at low significance, giving an estimated flux density of ≈0.06 mJy (from one flux-calibrated observation). Given the limited number of observations at frequencies other than 1400 MHz, accurate calculation of the spectral index was not possible. Observations at all three frequencies taken on the same day (with S/N of 3.2,[5] 13.6, and 9.0 at 700, 1400, and 3100 MHz, respectively) imply a spectral index of ≈−0.5, although this is subject to bias due to scintillation.

3 SYSTEM PARAMETERS

Using the TEMPO2 software package (Hobbs, Edwards & Manchester 2006) with the 'ELL1' binary model (Wex, unpublished), the combined data from Parkes and JBO result in a weighted rms timing residual of 7.2 μs. The timing data and resulting parameters are available in the online journal. Table 2 shows the parameters of the timing solution covering the entire data span, with the nominal 1σ uncertainties resulting from the fit. The derived parameters are also reported. 2σ upper limits are determined for the time derivatives of orbital period ($\dot{P}_b$) and projected semimajor axis ($\dot{x}$) by fitting for the parameters individually to determine the uncertainties. The 'ELL1' binary model uses the epoch of ascending node, T_{ASC}, and the first and second Laplace–Lagrange parameters, $\epsilon_1 = e\sin(\omega)$ and $\epsilon_2 = e\cos(\omega)$, where e is the eccentricity and ω is the orbital longitude. Fig. 2 shows the effect of the binary orbit in the timing residuals.

3.1 Astrometry

From the timing parallax of 4.4 ± 1.2 mas, we infer a distance of only 230^{+90}_{-50} pc. That is the reference value used throughout this paper as the correction for the Lutz–Kelker bias (220^{+100}_{-50} pc according to the formula in Verbiest et al. 2012) is negligible given the current uncertainty on the parallax. On the other hand, the latest electron density model, YMW16 (Yao et al. 2017), suggests a distance of 760 pc. Using the NE2001 model (Cordes & Lazio 2002), we find $d = 320$ pc, which is consistent with the parallax distance, whereas the YMW16 distance is not. Typical uncertainties for DM-derived distances are ∼20–30 per cent. The magnitude of this discrepancy in the electron density models is not uncommon for nearby pulsars.

As of 2017 May, the parallax measurement is significant at the >3σ level, but continued timing will allow for improved precision. At a distance of 230 pc, J2322−2650 is closer than all but seven pulsars (one MSP) with consistent distance measurements.[6] The 2σ upper limit on the parallax value gives a lower limit on the distance of 150 pc.

The total proper motion, from timing, is $\mu_{Tot} = 8.6(4)$ mas yr^{-1}, which, combined with the parallax distance, gives a transverse velocity of 10(3) km s^{-1}. Converting this to the local standard of rest yields a transverse velocity of 20(5) km s^{-1}.

[2] http://www.atnf.csiro.au/research/multibeam/lstavele/description.html
[3] CASPER Parkes Swinburne Recorder; http://www.astronomy.swin.edu.au/pulsar/?topic=caspsr.
[4] https://casper.berkeley.edu/wiki/ROACH

[5] The non-detection at 700 MHz was scaled to a S/N of 5.0 to calculate the upper limit on the flux density for the spectral index.
[6] 'Consistent' distances, from the ATNF Pulsar Catalogue, are those from timing parallax or independent distance measurements, or where the YMW16 and NE2001 models agree within a factor of 3: 2396 pulsars (139 MSPs) total.

Table 2. Pulsar parameters from radio timing using TEMPO2 – uncertainties on direct timing parameters from TEMPO2

Parameter	Value
Right ascension, RA (J2000) ($^{h}:^{m}:^{s}$)	23:22:34.64004(3)
Declination, Dec. (J2000) ($^{\circ}:':''$)	−26:50:58.3171(6)
Period, P (s)	0.00346309917908790(11)
Period derivative, $\dot{P}$ (s s^{-1})	$5.834(15) \times 10^{-22}$
Period epoch[a] (MJD)	56152.0
DM (pc cm^{-3})	6.149(2)
Parallax (mas)	4.4(12)
Proper motion in RA (mas yr^{-1})	−2.4(2)
Proper motion in Dec. (mas yr^{-1})	−8.3(4)
Binary model	ELL1
P_b (d)	0.322963997(6)
T_{ASC} (MJD)	56130.35411(2)
x (lt-s)	0.0027849(6)
ϵ_1	−0.0002(4)
ϵ_2	0.0008(4)
$\dot{P}_b$[b] (s s^{-1})	$\lesssim 6 \times 10^{-11}$
$\dot{x}$[b] (lt-s s^{-1})	$\lesssim 3 \times 10^{-14}$
Data span (yr)	4.8
Weighted rms residual (μs)	7.3
Number of TOAs	338
S_{1400} (mJy)	0.16(2)
FWHM at 1.4 GHz (ms)	0.11(1)
Derived parameters	
B_{surf} (G)	$4.548(12) \times 10^{7}$
Parallax-derived distance (kpc)	$0.23^{+0.09}_{-0.05}$
DM-derived distance[c] (kpc)	0.76
μ_{Tot} (mas yr^{-1})	8.6(4)
V_{trans}[d] (km s^{-1})	20(5)
$\dot{P}_{int}$[e] (s s^{-1})	$4.4(5) \times 10^{-22}$
$\dot{E}_{int}$ (erg s^{-1})	$4.2(4) \times 10^{32}$
e[b]	$\lesssim 0.0017$
ω ($^{\circ}$)	333(27)
Predicted $\dot{\omega}$[f] (deg yr^{-1})	1.6
Mass function ($M_{\odot}$)	$2.229(1) \times 10^{-10}$
Min. companion mass[f] ($M_{\odot}$)	0.0007588(2)
Min. companion density (g cm^{-3})	1.84
L_{1400}[e] (mJy kpc^2)	0.008(5)

Notes. [a]Period epoch also used as position epoch and DM epoch.
[b]2σ upper limit.
[c]YMW16 model (Yao, Manchester & Wang 2017).
[d]With respect to the local standard of rest.
[e]Using parallax-derived distance.
[f]Assuming a pulsar mass of 1.4 $M_{\odot}$.

3.2 Intrinsic properties

Our timing yields an observed period derivative of $\dot{P}_{obs} = 5.834(15) \times 10^{-22}$ s s^{-1}, which implies a magnetic field strength of just $B_{surf} = 4.55(1) \times 10^{7}$ G (where the given uncertainty does not take into account the assumptions made in the derivation). Correcting for the Shklovskii effect (ignoring the negligible contribution of the Galactic potential), we find an intrinsic period derivative of $\dot{P}_{int} = 4.4(5) \times 10^{-22}$ s s^{-1}. This is the lowest, significant intrinsic $\dot{P}$ currently known after correcting for the Shklovskii effect, with the uncertainty derived from the large uncertainty on the parallax distance and the small uncertainty on the observed period derivative. If we assume $\dot{P}_{int}$ must be positive, the distance is constrained to be $\lesssim 0.9$ kpc. The 2σ upper limit from the parallax corresponds to a distance of >150 pc and $\dot{P}_{int,max} = 4.9 \times 10^{-22}$ s s^{-1}.

Using the optimal value for $\dot{P}_{int}$, we find $B_{surf,i} = 4.0(5) \times 10^{7}$ G. Fig. 3 compares periods and magnetic field strengths of known MSPs, corrected for secular acceleration. MSPs in globular clusters have been excluded due to the dominant effect of gravitational acceleration from their environments. Note some field MSPs have negative period derivatives when corrected for the Shklovskii effect, largely due to contributions of the Galactic potential, and are therefore excluded from this figure. J2322−2650 has the lowest intrinsic magnetic field strength of the remaining field MSPs. The other pulsars with planetary-mass companions have magnetic field strengths comparable with the other field MSPs with similar periods. As noted in Table 2, the intrinsic spin-down luminosity of J2322−2650 is $\dot{E}_{int} = 4.2(4) \times 10^{32}$ erg s^{-1}.

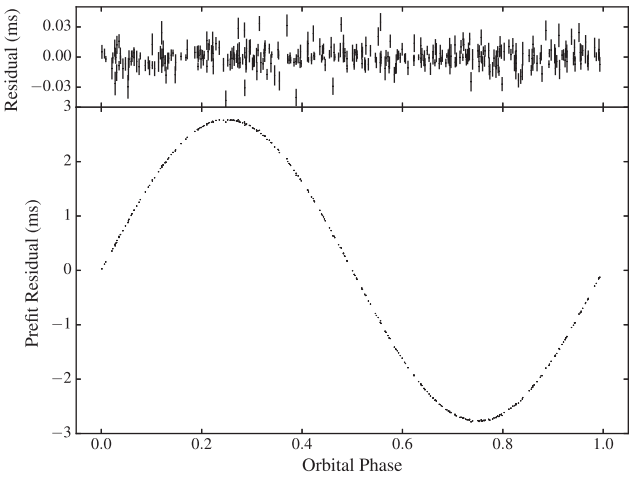

Figure 2. Upper panel: pulse timing residuals for J2322−2650 with the optimal parameters (listed in Table 2). Lower panel: residuals before fitting for the semimajor axis, demonstrating the effect of the binary motion. There is no significant orbital eccentricity, nor is there evidence for eclipses or excessive dispersive delays at superior conjunction of the pulsar (orbital phase 0.25).

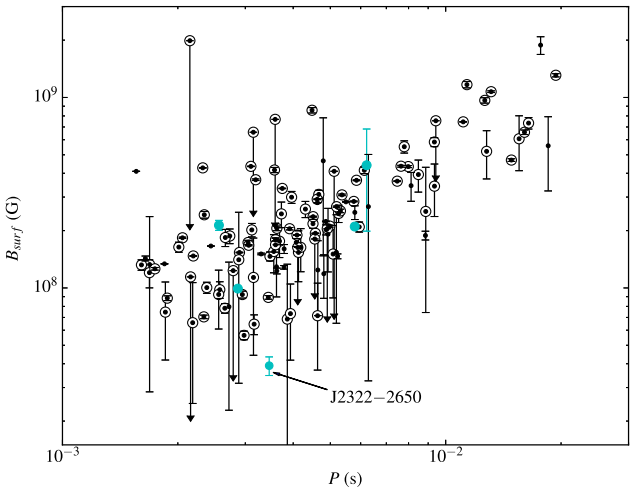

Figure 3. Intrinsic magnetic field strength versus period for field MSPs (data from the ATNF Pulsar Catalogue, v1.56). Black circles around dots indicate binary systems (with 1σ uncertainties), and dots alone indicate isolated systems. 1σ upper limits are used for pulsars with poorly constrained distance and proper motion measurements. The MSPs with planetary-mass companions are shown by the filled cyan circles. J2322−2650 is annotated, lying lower than MSPs with comparable periods, with 2σ uncertainties.

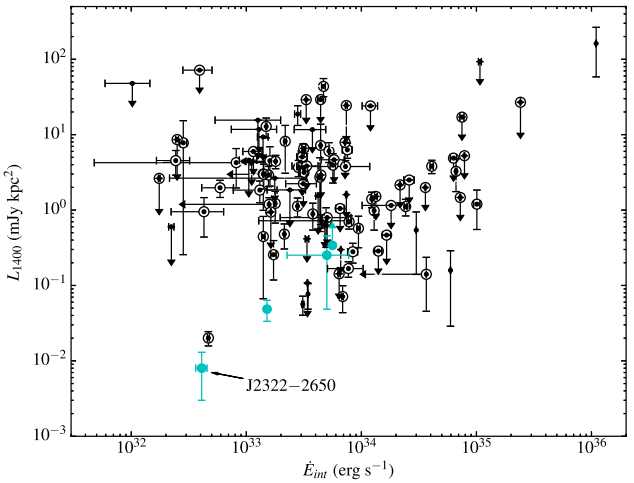

Figure 4. Radio luminosity versus intrinsic spin-down luminosity for MSPs in the field (data from the ATNF Pulsar Catalogue, v1.56). Black circles around dots indicate binary systems (with 1σ uncertainties), and dots alone indicate isolated systems. 1σ upper limits are used for pulsars with poorly constrained distance and proper motion measurements. The MSPs with planetary-mass companions are shown by the filled cyan circles. J2322−2650 is annotated, with the lowest radio luminosity.

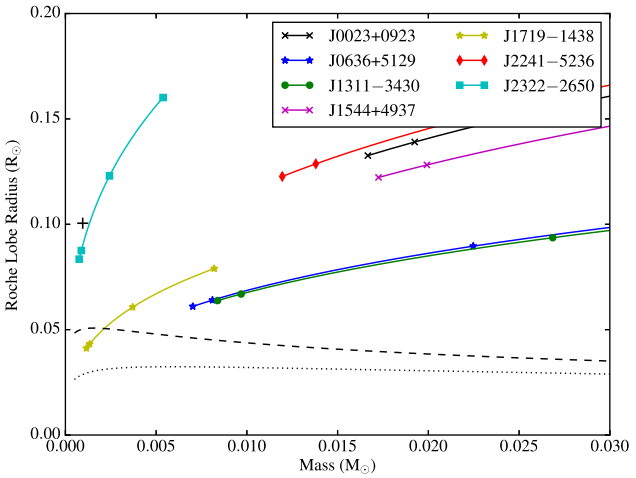

Figure 5. Plot of maximum Roche lobe radii versus companion mass for field MSPs with companions with very low masses ($x < 0.04$ lt-s and $m_{\rm min} < 0.02\,{\rm M}_\odot$). The points from lowest to highest mass represent the maximum ($i = 90°$), median ($i = 60°$), 5 per cent ($i = 18.^\circ2$), and 1 per cent ($i = 8.^\circ1$) probabilities for the system inclination angle. The dashed and dotted lines indicate the mass–radius relations for low-mass He and C white dwarfs, respectively, by Eggleton (Rappaport et al. 1987). For reference, the mass and radius of Jupiter are marked with a cross.

3.3 Energetics

As noted in Section 2.2, the mean flux density of J2322−2650 at 1400 MHz is $S_{1400} = 0.16(2)$ mJy, so the radio luminosity of the source is $L_{1400} = 0.008(5)$ mJy kpc^2 (using the parallax-derived distance). This, too, is highly dependent on the distance measure. At the parallax-derived distance of 230 pc, the luminosity is lower than all consistent published values.[7] Fig. 4 shows a comparison of radio luminosity and intrinsic spin-down luminosity for field MSPs with directly measured 1400 MHz flux density and reliable distance measurements. We distinguish binary and isolated systems in the figure, but note no obvious difference between these populations, or correlation between the quantities, in this comparison. Of the pulsars with planetary-mass companions, PSR J1311−3430 is not plotted in this figure as the 1400 MHz flux density has not been measured, and PSR J0636+5128 is plotted at the lower limit of the luminosity from the timing parallax (see Section 4.2).

3.4 Binary parameters

From the binary period, $P_{\rm b} = 0.322963997(6)$ d, and projected semimajor axis, $x = 0.0027849(6)$ lt-s, we find the mass function of J2322−2650 is $2.23 \times 10^{-10}\,{\rm M}_\odot$, so the minimum companion mass is $M_{\rm c,\,min} = 0.000759\,{\rm M}_\odot$, assuming a pulsar mass of $m_{\rm p} = 1.4\,{\rm M}_\odot$. For lower inclination angles and higher pulsar masses, the companion mass increases, but remains below $0.01\,{\rm M}_\odot$ for $m_{\rm p} \leq 2.0\,{\rm M}_\odot$ and $i \geq 8.^\circ1$ (99 per cent probability given random system orientations). From the binary period, $P_{\rm b}$, we calculate the minimum density of the companion (Frank, King & Raine 1985):

$$\rho = \frac{3\pi}{0.462^3 G P_{\rm b}^2} = 1.83\,{\rm g\,cm^{-3}}. \quad (1)$$

In Fig. 5, we plot the relation between the Roche lobe radius and the mass of the companion for binary MSPs in the Galactic field with light companions (i.e. having a minimum companion mass smaller than $0.02\,{\rm M}_\odot$). Each line in the plot covers the 99 per cent most probable orbital inclinations for any given MSP binary. We note that the range of masses and radii for J2322−2650 is comparable to the mass and radius of Jupiter.

No post-Keplerian or higher order binary parameters have been required in the parameter fits (see Section 3). The advance of periastron, $\dot{\omega}$, cannot be included in the parameter fits, but the value from relativistic effects can be calculated assuming a pulsar mass of $1.4\,{\rm M}_\odot$, giving $\dot{\omega}_{\rm min} \approx 1.^\circ6\,{\rm yr}^{-1}$, which is not likely measurable due to the extremely low eccentricity of the orbit.

We see no evidence for delays in the timing at superior conjunction of the pulsar. This implies that there is no excess material in the system, or that the inclination of the system with respect to the line of sight prevents such material from affecting the delays of the pulsar signal.

3.5 Multiwavelength observations

We searched archives of *Fermi*, *Chandra*, and *XMM–Newton* missions for counterparts at other wavelengths. No observations within 10 arcmin of the radio position were found in *Chandra* or *XMM–Newton* archives. The *Fermi* Large Area Telescope (LAT) 4-yr Point Source Catalogue (Acero et al. 2015) listed no sources within 30 arcmin . An attempt to detect the pulsations using our ephemeris and the entire *Fermi* data set was not successful (Kerr private communication). From fig. 17 in Abdo et al. (2013), we estimate the upper limit on the flux density from 0.1 to 100 GeV at a Galactic latitude of $b = -70°$ to be $\lesssim 3 \times 10^{-12}$ erg s^{-1} cm^{-2}, which would correspond to a luminosity of $L_\gamma \lesssim 2 \times 10^{31}$ erg s^{-1}. The implied γ-ray efficiency[8] is therefore $\eta_\gamma \lesssim 5 \times 10^{-2}$, which is consistent with MSPs detected in that energy range, as shown in Abdo et al. (2013).

[7] Again, using ATNF catalogue sources with consistent distance measurements, and measured flux density at 1400 MHz; 1684 pulsars (120 MSPs).

[8] η_γ is defined as the ratio of L_γ and $\dot{E}_{\rm int}$.

J2322−2650 is also undetected in a ∼1700-s observation (PI: J. L. Linsky, ROR 200461) performed on 1991 November 20 (UT 22:11) with the *ROSAT* Position Sensitive Proportional Counter (PSPC; Pfeffermann, Briel & Freyberg 2003) targeting HR 8883, a star located ≈19 arcmin from the radio position of J2322−2650. We reanalysed this *ROSAT* pointing using standard tools. In order to establish an upper limit to the observed X-ray flux, the analysis accounted for (i) the offset from the centre of the field of view, and (ii) the expected low X-ray absorption column density towards the source (estimated using the Leiden/Argentine/Bonn Survey of Galactic H I; Kalberla et al. 2005). We also (iii) assumed a power-law spectrum, exploring photon indices around −2, which is often applied for inferring upper limits to the non-thermal X-ray emission from radio pulsars (e.g. Becker 2009). The result was a 3σ upper limit to the unabsorbed X-ray flux of $\sim 2 \times 10^{-13}$ erg cm^{-2} s^{-1} in the 0.1–2.4 keV band. Since there is evidence for predominantly thermal X-ray emission from MSPs with intrinsic spin-down power $\dot{E}_{\rm int} \lesssim 10^{35}$ erg s^{-1} (see e.g. Kargaltsev et al. 2012), the consequences of the assumption of a blackbody spectrum were also explored. For surface temperatures in the range 0.5–5 $\times$ 10^6 K (reflecting what is typically observed in the MSP sample), an upper limit on the unabsorbed X-ray flux similar to the one above was obtained. This limit corresponds to an isotropic X-ray luminosity $L_{[0.1-2.4\,{\rm keV}]} \lesssim 10^{30}\,{\rm erg\,s^{-1}}(\frac{d}{230\,{\rm pc}})^2$ in the *ROSAT* PSPC band, where d is the distance of the J2322−2650 binary, and the luminosity is scaled to the timing parallax distance. The implied upper limit to the X-ray efficiency[9] of the pulsar, $\eta_{\rm X} \sim 2 \times 10^{-3}(\frac{d}{230\,{\rm pc}})^2$, agrees with what is seen in the bulk of the MSP population (e.g. Possenti et al. 2002; Becker 2009; Kargaltsev et al. 2012).

If we assume emission from the pulsar is heating the companion, we can estimate the expected blackbody temperature and optical brightness of the system. We assume a certain geometry for the system: that the orbit is edge-on (the most likely and optimistic orientation for detection) and that the companion is tidally locked and filling its Roche lobe. As shown in Section 3.4, the system has an orbital period of $P_{\rm b} \approx 0.322964$ d and projected semimajor axis of $x = a_1 \sin i \approx 0.002785$ lt-s, and, therefore, the minimum companion mass is $m_{\rm c} \approx 0.000759\,{\rm M}_\odot$. From Kepler's Third Law, because $m_{\rm c} \ll m_{\rm p}$, to a high degree of accuracy the system separation is

$$a = 4.208\,{\rm R}_\odot \left(\frac{P_{\rm b}}{\rm d}\right)^{2/3} \left(\frac{m_{\rm p}}{{\rm M}_\odot}\right)^{1/3} = 2.2\,{\rm R}_\odot. \quad (2)$$

From this, the Roche lobe radius of the companion (Paczyński 1971) is

$$R_{\rm L} = 0.462\,a \left(\frac{m_{\rm c}}{m_{\rm c}+m_{\rm p}}\right)^{1/3} = 0.083\,{\rm R}_\odot. \quad (3)$$

If the spin-down power, $\dot{E} \approx 4.2 \times 10^{32}$ erg s^{-1}, is emitted isotropically, the minimum blackbody temperature of the companion is $T_{\rm eff} \approx 2300$ K. This would result in an apparent visual magnitude of $V \approx 28$ mag at system quadrature, and $V \approx 27$ mag at inferior conjunction of the pulsar. At the position ($l = 23.^\circ64$, $b = -70.^\circ23$) and estimated distance of the system, we estimate the absorption to be $E(B-V) \approx 0.01 \pm 0.03$ mag, following Green et al. (2015),[10] which is negligible. Given the low $T_{\rm eff}$ of the companion, we use the relations found by Reed (1998) and Casagrande, Flynn & Bessell (2008) for cool M dwarfs to estimate $V - R \approx 2$, implying a magnitude of $R \approx 26$ mag at quadrature ($R \approx 25$ mag at inferior conjunction).

[9] $\eta_{\rm X}$ is defined as the ratio of $L_{[0.1-2.4\,{\rm keV}]}$ and $\dot{E}_{\rm int}$.
[10] http://argonaut.skymaps.info/.

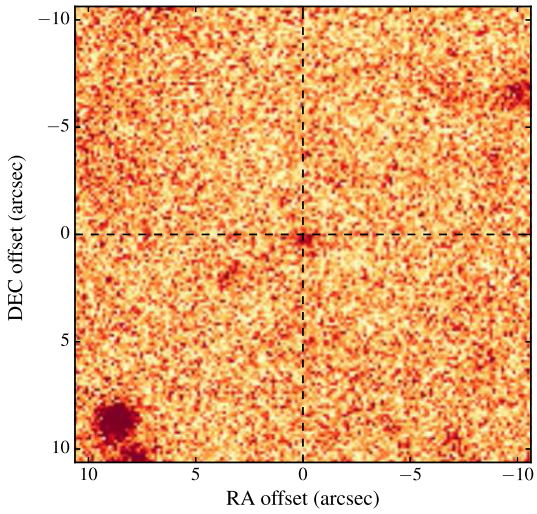

Figure 6. An image from the (summed) 1500 s observation with the Keck DEIMOS instrument in *R* band. The axes indicate the offset from the radio pulsar position, with the black dashed lines denoting zero offset in RA and Dec. The centroid of the possible counterpart is ∼0.6 arcsec from the radio position.

In an attempt to detect the companion, we took three 500 s exposures with the Keck Deep Imaging Multi-Object Spectrograph (DEIMOS) instrument in *R* band on 2016 September 8, as shown in Fig. 6. We detect an optical source 0.6 arcsec from the radio position (with 0.3 arcsec uncertainty in the astrometry) with an apparent *R*-band magnitude of 26.4 ± 0.2, where the uncertainty is given by Source Extractor (SExtractor; Bertin & Arnouts 1996), and we estimate systematic error of up to 0.2 mag may also be present. The seeing of the observation was ≈1.1 arcsec, estimated from stellar sources in the field of view, and the limiting magnitude is ≈25.8 mag (completeness limit). We estimate the probability of a random alignment of the radio position with an optical source as 4 per cent for sources down to $R \approx 25.8$ mag. Therefore, the association of the optical and radio sources is approximately at the 2σ confidence level. The observation commenced at orbital phase ≈0.75 (inferior conjunction of the pulsar) for which our estimate of the blackbody emission results in an *R*-band magnitude of ≈25. Further observations at a range of orbital phases and better astrometry will ultimately determine whether the 26.4 mag source is indeed the planetary-mass companion to J2322−2650.

4 DISCUSSION

4.1 Population statistics

One of the most striking properties of J2322−2650 is its low luminosity of 0.008(5) mJy kpc^2. Low-luminosity MSPs appear in surveys relatively rarely unless their Galactic population is very large, and in this section we explore what fraction of the total MSP population might resemble J2322−2650, cognizant of the fact that we are basing our discussion on just one object.

In order to compare the Galactic population of J2322−2650-like pulsars to the Galactic MSP population, a thorough analysis of the selection biases in our survey is necessary. To this end, we

use the PSREVOLVE software[11] to simulate a specified number of pulsars scattered throughout the galaxy with assumed spatial distribution and distribution of pulsar parameters (period, magnetic field, luminosity, intrinsic pulse width) and determine if each pulsar would be detected in certain pulsar surveys. As detailed in Levin et al. (2013), the simulation distributes pulsars at Galactic positions using a radial Gaussian distribution with radial scale length $R = 4.5$ kpc, centred on the Galactic Centre, and a vertical Gaussian distribution with scale height $z = 500$ pc. A data base of the coordinates of observations for the HTRU high-latitude survey is used to define the survey region. If the simulated pulsar is within the survey region, the pulse width (accounting for scattering and dispersion smearing) is calculated. If the pulse width is less than the pulse period, the final condition for detection (the flux density of the pulsar compared with the flux density limit of the survey) is checked. For each simulation run, we simulated $\sim 5 \times 10^5$ pulsars with the period, magnetic field strength, luminosity, and pulse width of J2322−2650 and checked how many were 'detected' in the high-latitude survey. The number of pulsars simulated normalized by the number of pulsars 'detected' provides a scaling factor: the total number of J2322−2650-like MSPs in the galaxy beaming towards the Earth. The simulation does not take into account the evolution or formation of MSPs and binary systems, so this analysis merely estimates the current population of low-luminosity MSPs in the galaxy.

PSREVOLVE uses the NE2001 DM–distance model, so, for consistency, we used as input the luminosity of J2322−2650 at the NE2001 distance of 320 pc ($L_{1400} = 0.016$ mJy kpc^2). Out of 20 runs, we found a mean scaling factor of 9×10^4 with a standard deviation of 5×10^4. We also simulated a brighter pulsar ($L_{1400} = 0.16$ mJy kpc^2; all other parameters identical to J2322−2650) and found a scaling factor of $3.2(9) \times 10^3$. The ratio of J2322−2650-like MSPs to those with an order of magnitude higher luminosity is, therefore, 28 ± 18, which is consistent with the slope of the luminosity distribution found by Levin et al. (2013): $(\mathrm{d}\log N/\mathrm{d}\log L) = -1.45 \pm 0.14$.

We have also used the PSRPOPPY software package (Bates et al. 2014) to confirm our results, using identical spatial distributions and pulsar parameters. With this software, we find a scaling factor of $(3.7 \pm 0.8) \times 10^4$ for J2322−2650-like MSPs and (1650 ± 90) for the higher luminosity MSPs, and therefore a ratio of 23 ± 5 for the populations. The PSREVOLVE software includes a rough model of the effects of RFI on the surveys, thereby decreasing the detection likelihood and increasing the scatter in the scaling factors for the runs. Neither simulation tool accounts for refractive scintillation, which would affect the rate of detection of nearby pulsars such as J2322−2650. These results also do not reflect the expected uncertainties from Poisson statistics. With this analysis, we do not claim a significant determination of the total population of low-luminosity MSPs. Rather, the detection of even a single low-luminosity MSP may imply the existence of a population of such MSPs that may dominate the Galactic MSP population.

4.2 Comparison with other known MSP binaries

If MSPs that are recycled by stars that leave behind planetary-mass companions have systematically low radio luminosities, we might expect to see that reflected in other members of the population. Below we discuss this population of MSPs, with properties summarized in Table 3.

Table 3. Pulsars with low-mass companions – comparison of companion masses, and radio luminosities and efficiencies.

Pulsar	M_c (M_J)	L_{1400} (mJy kpc^2)	$\dot{E}_{int}$ ($\times 10^{33}$ erg s^{-1})	ϵ ($\times 10^{-7}$)
J0636+5128	7.2	>0.34	5.60(6)	4.6
B1257+12[a]	0.014	≈0.3	5(3)	6.0
J1311−3430	8.6	≈0.22	41(3)[b]	0.3
J1719−1438	1.2	≈0.049[c]	1.52(5)	2.3
J2322−2650	0.76	0.008(5)	0.42(4)	1.3

Notes. [a]The mass of planet A is listed for B1257+12.
[b]No proper motion measured for J1311−3430; $\dot{P}_{int}$ is approximated from the measured $\dot{P}$.
[c]Radio luminosity using the YMW16 distance.

Besides J2322−2650, the only MSPs with planetary-mass companions are PSRs J0636+5128, B1257+12, J1311−3430, and J1719−1438. We note that PSR B1620−26 also has a planetary-mass companion, but this system is in a globular cluster, and is therefore not directly comparable to J2322−2650.

J0636+5128 is a low-mass Black Widow systems (with no radio eclipses) with a $7.2\,M_J$ companion in a 1.60 h orbit (Stovall et al. 2014; therein referred to as J0636+5129).[12] Stovall et al. (2014) discuss the possibility that this system was formed via runaway mass transfer and ablation, noting that there is no sign of excess material in the orbit from radio observations. The MSP has a mean flux density of $S_{1400} = 0.69$ mJy and a lower limit on the distance of >700 pc (from the NANOGrav 11-yr Data Release; Arzoumanian et al., in preparation), implying a radio luminosity of >0.34 mJy kpc^2. The intrinsic spin-down luminosity of the pulsar is also not unusually low, at $5.60(6) \times 10^{33}$ erg s^{-1}.

B1257+12 has three companions with masses in the range of 6.3×10^{-5}–$1.35 \times 10^{-2}\,M_J$ with orbital periods of 25–98 d (Wolszczan & Frail 1992; Konacki & Wolszczan 2003). Wolszczan (1997) conclude that the planets likely formed in an accretion disc during or after the transfer of matter from the original (stellar) companion on to the pulsar. The MSP has a mean flux density at 1400 MHz of ≈0.5 mJy (from P140 Parkes observations) and a parallax distance of 0.71(4) kpc (Yan et al. 2013), which implies a radio luminosity of ≈0.3 mJy kpc^2. Similar to J0636+5128, B1257+12 has an intrinsic spin-down luminosity of $\dot{E}_{int} = 5(3) \times 10^{33}$ erg s^{-1}.

J1311−3430 is another low-mass Black Widow system, first detected in a *Fermi* blind search, and has an $8.6\,M_J$ companion in a 1.57 h orbit (Pletsch et al. 2012). This MSP is in an eclipsing system where the pulsar is ablating its companion with a high-energy wind (Pletsch et al. 2012), and may therefore be similar to the progenitors of J0636+5128 and J1719−1438. J1311−3430 was initially detected as a γ-ray source, and has only been detected in radio frequencies once (Ray et al. 2013), implying a flux density at that time of $S_{1400} \approx 0.11(6)$ mJy. The DM–distance from this detection is 1.4(1) kpc, which thus implies a radio luminosity of ≈0.22 mJy kpc^2. It has a significantly higher $\dot{E}_{int}$ (approximated from the observed $\dot{P}$ as no proper motion has been measured) than the other low-mass pulsar systems, $4.1(3) \times 10^{34}$ erg s^{-1}, and the observed ablation of its companion is assumed to be a consequence of that energy loss.

[11] Developed by F. Donea and M. Bailes, based on work by D. Lorimer. http://astronomy.swin.edu.au/fdonea/psrevolve.html.

[12] See Footnote 1.

J1719−1438 has a $1.2\,M_J$ companion in a 2.2 h orbit (Bailes et al. 2011). Like J0636+5128, J1719−1438 is a possible case of ablation due to an energetic wind (Bailes et al. 2011), although no excess material is now observable. For J1719−1438, there is some ambiguity in the distance from the DM, with YMW16 giving a value of 0.34(3) kpc and NE2001 giving 1.2(3) kpc, and, as of 2017 May, there is no published parallax value. Combined with a flux density of $S_{1400} = 0.42$ mJy (Ng et al. 2014), the YMW16 (NE2001) distance estimate implies a radio luminosity of $\approx$0.049 mJy kpc^2 ($\approx$0.61 mJy kpc^2).

In comparison with the other MSPs with planetary-mass companions, J2322−2650 most closely resembles J0636+5128 and J1719−1438, with similar companion masses and spin-down luminosities. The spin-down luminosity of J2322−2650 is lower than the mean of the MSP population (Fig. 4), although the other MSPs with planetary-mass companions have more typical luminosities.

It is interesting to note that Burgay et al. (2013), as well as previous studies by Kramer et al. (1998) and Bailes et al. (1997), found that isolated MSPs and binary MSPs have different intrinsic luminosity functions, where isolated MSPs have lower luminosities on average than MSPs with companions. They suggest the difference may reflect differing evolutionary histories for the two populations. However, in recent years, additional isolated MSPs with average or high luminosities have been discovered, such as PSRs J1747−4036 (Kerr et al. 2012; Camilo et al. 2015) and J1955+2527 (Deneva et al. 2012), which do not support a significant difference between the luminosities of the two populations. At the YMW16 distance, J1719−1438 has a radio luminosity comparable to that of J2322−2650, which is significantly less than the median radio luminosity for binary MSPs.[13] B1257+12 differs significantly from the other pulsars with planetary-mass companions with a higher radio luminosity and multiple Earth-mass companions, and we expect this is due to a different formation scenario from the other systems (discussed below).

As shown in Table 3, if we assume a beaming fraction of 1, the radio efficiencies of these pulsars, $\epsilon = L_r/\dot{E}_{\rm int}$, where L_r is the radio luminosity at 1400 MHz in erg s^{-1}, are comparable. The remainder of the known MSPs have a mean (median) efficiency of 4×10^{-5} (3×10^{-6}), with no significant difference between the distributions for isolated and binary MSPs.

4.3 Formation scenarios

The possible formation scenarios for this system are, as above: planet formation around the main-sequence progenitor to the pulsar, planet formation in a supernova fallback disc, and the evaporation or ablation of the original companion to an extremely low mass. Following Miller & Hamilton (2001), we consider it highly unlikely for the planet to have formed around the main-sequence star and remained bound after the supernova event.

Kerr et al. (2015) have searched for periodicity in timing data for 151 young pulsars to place limits on the existence of planets around pulsars. They find that planet formation within $\approx$1.4 au is a rare phenomenon, so it is unlikely that the companion to J2322−2650 formed before the pulsar was recycled.

An alternative scenario is the formation of the planetary-mass companion in the accretion disc from the original companion, and subsequent loss of the original companion. Alpar et al. (1982) define the accretion time as

$$T_a \sim 1.4 \times 10^8\,{\rm yr} \left(\frac{M}{{\rm M}_\odot}\right)^{-2/3} \left(\frac{P}{\rm ms}\right)^{-4/3} I \dot{m}_{17}^{-1}, \quad (4)$$

where I is the moment of inertia in units of 10^{45} g cm^2 and $\dot{m}_{17}$ is the accretion rate in units of 10^{17} g s^{-1}, yielding an accretion time of $\sim 2 \times 10^7$ yr for a pulsar mass of $1.4\,{\rm M}_\odot$, period of 3.46 ms, and $\dot{m}_{17} = 1 \times 10^{17}$ g s^{-1}. Hansen, Shih & Currie (2009) discuss the formation of Earth-mass planets in discs and find that such bodies form in $\sim 10^7$ yr, but their simulations do not form Jupiter-mass objects. Although we cannot completely reject this formation scenario, it is not our preferred model.

Given the similarities between J2322−2650, J0636+5128, and J1719−1438, it is possible that the planetary-mass companion we now observe is the remnant of the original companion after runaway mass transfer. Following Alpar et al. (1982), the formation of a pulsar with a period of 3.46 ms would require $\sim$0.05 M$_\odot$ transferred from an evolved companion, assuming a final pulsar mass of $1.4\,{\rm M}_\odot$. The minimum density of the companion is 1.83 g cm^{-3}, which does not preclude a scenario where the original companion transferred material to the pulsar and was ablated by the pulsar wind, reducing the companion to a mass of $\approx$0.0008 M$_\odot$. Stevens, Rees & Podsiadlowski (1992) describe an ablation scenario by relating the mass loss of the companion, $\dot{M}_2$, to the energy loss of the pulsar, L_p, as

$$\dot{M}_2 \propto L_p \left(\frac{R_2}{a}\right)^2, \quad (5)$$

where R_2 is the radius of the companion and a is the separation. We can compare J2322−2650 with PSR B1957+20, a Black Widow ablating its companion at a rate of $\dot{M}_2 \sim 3 \times 10^{16}$ g s^{-1} (Applegate & Shaham 1994). J2322−2650 has a lower spin-down luminosity, so equation (5) implies a mass-loss rate of just $\sim 10^{13}$ g s^{-1}. At this rate, the companion to J2322−2650 would lose just $0.1\,M_J$ in $\sim 10^9$ yr. The high-luminosity, isolated MSP, PSR B1937+21, with its high spin-down luminosity $\dot{E}_{\rm int} = 1.1 \times 10^{36}$ erg s^{-1}, with the same orbital parameters as J2322−2650, would ablate the entire companion in only $\sim 10^6$ yr. Therefore, we speculate that J2322−2650 has a planetary-mass companion remaining due to its low spin-down luminosity, and that a more energetic pulsar with an identical original companion would destroy its companion and become isolated.

5 CONCLUSIONS

In this paper, we have presented the discovery of an MSP unlike other known MSPs: a nearby MSP, characterized by a low surface magnetic field strength and a low radio luminosity, with a low-density, planetary-mass companion. A single observation of the system with the Keck DEIMOS instrument in R band revealed a source of $R \approx 26.4(4)$ mag that is associated with the pulsar companion at the 2σ confidence level.

If MSPs with planetary-mass companions have luminosities similar to J2322−2650, they may dominate the galactic MSP population. Future surveys with telescopes like the Square Kilometre Array (SKA) and Five-hundred-meter Aperture Spherical radio Telescope (FAST) may reveal them.

ACKNOWLEDGEMENTS

We thank I. Andreoni for his assistance with reduction of the optical data, and P. Esposito for his advice regarding the X-ray data analysis.

[13] See Footnote 7.

We also thank the anonymous referee for useful comments that significantly improved the paper. This research was funded partially by the Australian Government through the Australian Research Council, grants CE170100004 (OzGrav) and FL150100148. MK's research is supported by the ERC Synergy Grant 'BlackHoleCam: Imaging the Event Horizon of Black Holes' (Grant 610058). The Parkes radio telescope is part of the Australia Telescope National Facility that is funded by the Australian Government for operation as a National Facility managed by CSIRO. Pulsar research at the Jodrell Bank Centre for Astrophysics and the observations using the Lovell Telescope are supported by a consolidated grant from the STFC in the UK. Some of the data presented herein were obtained at the W.M. Keck Observatory, which is operated as a scientific partnership among the California Institute of Technology, the University of California, and the National Aeronautics and Space Administration. The Observatory was made possible by the generous financial support of the W.M. Keck Foundation. This work used the gSTAR national facility that is funded by Swinburne and the Australian Government's Education Investment Fund. This research made use of ASTROPY, a community-developed core PYTHON package for Astronomy (Astropy Collaboration, 2013), and the MATPLOTLIB package (v1.5.1; Hunter 2007).

REFERENCES

Abdo A. A. et al., 2013, ApJS, 208, 17
Acero F. et al., 2015, ApJS, 218, 23
Alpar M. A., Cheng A. F., Ruderman M. A., Shaham J., 1982, Nature, 300, 728
Applegate J. H., Shaham J., 1994, ApJ, 436, 312
Backer D. C., Kulkarni S. R., Heiles C., Davis M. M., Goss W. M., 1982, Nature, 300, 615
Bailes M. et al., 1997, ApJ, 481, 386
Bailes M. et al., 2011, Science, 333, 1717
Barr E. D. et al., 2013, MNRAS, 435, 2234
Bassa C. G. et al., 2016, MNRAS, 456, 2196
Bates S. D., Lorimer D. R., Rane A., Swiggum J., 2014, MNRAS, 439, 2893
Becker W., 2009, in Becker W., ed., Astrophysics and Space Science Library, Vol. 357, Neutron Stars and Pulsars. Springer-Verlag, Berlin, p. 91
Bertin E., Arnouts S., 1996, A&AS, 117, 393
Bisnovatyi-Kogan G. S., Komberg B. V., 1976, Soviet Astron. Lett., 2, 130
Burgay M. et al., 2003, Nature, 426, 531
Burgay M. et al., 2013, MNRAS, 433, 259
Camilo F. et al., 2015, ApJ, 810, 85
Casagrande L., Flynn C., Bessell M., 2008, MNRAS, 389, 585
Cordes J. M., Lazio T. J. W., 2002, preprint (arXiv Astrophysics:e-prints)
Deloye C. J., 2008, in Bassa C., Wang Z., Cumming A., Kaspi V. M., eds, AIP Conf. Proc. Vol. 983, 40 Years of Pulsars: Millisecond Pulsars, Magnetars and More. Am. Inst. Phys., New York, p. 501
Deneva J. S. et al., 2012, ApJ, 757, 89
Frank J., King A. R., Raine D. J., 1985, Accretion Power in Astrophysics. Cambridge Univ. Press, Cambridge
Green G. M. et al., 2015, ApJ, 810, 25
Hansen B. M. S., Shih H.-Y., Currie T., 2009, ApJ, 691, 382
Hewish A., Bell S. J., Pilkington J. D. H., Scott P. F., Collins R. A., 1968, Nature, 217, 709
Hobbs G. B., Edwards R. T., Manchester R. N., 2006, MNRAS, 369, 655
Hulse R. A., Taylor J. H., 1975, ApJ, 195, L51
Hunter J. D., 2007, Comput. Sci. Eng., 9, 90
Kalberla P. M. W., Burton W. B., Hartmann D., Arnal E. M., Bajaja E., Morras R., Pöppel W. G. L., 2005, A&A, 440, 775
Kargaltsev O., Durant M., Pavlov G. G., Garmire G., 2012, ApJS, 201, 37
Keith M. J. et al., 2010, MNRAS, 409, 619
Kerr M. et al., 2012, ApJ, 748, L2
Kerr M., Johnston S., Hobbs G., Shannon R. M., 2015, ApJ, 809, L11
Konacki M., Wolszczan A., 2003, ApJ, 591, L147
Kramer M., Xilouris K. M., Lorimer D. R., Doroshenko O., Jessner A., Wielebinski R., Wolszczan A., Camilo F., 1998, ApJ, 501, 270
Kramer M., Lyne A. G., O'Brien J. T., Jordan C. A., Lorimer D. R., 2006, Science, 312, 549
Levin L. et al., 2013, MNRAS, 434, 1387
Lyne A. G. et al., 2004, Science, 303, 1153
Manchester R. N., Hobbs G. B., Teoh A., Hobbs M., 2005, AJ, 129, 1993
Martin R. G., Livio M., Palaniswamy D., 2016, ApJ, 832, 122
Miller M. C., Hamilton D. P., 2001, ApJ, 550, 863
Ng C. et al., 2014, MNRAS, 439, 1865
Paczyński B., 1971, ARA&A, 9, 183
Pfeffermann E., Briel U. G., Freyberg M. J., 2003, Nucl. Instrum. Methods Phys. Res. A, 515, 65
Pletsch H. J. et al., 2012, Science, 338, 1314
Possenti A., Cerutti R., Colpi M., Mereghetti S., 2002, A&A, 387, 993
Rappaport S., Ma C. P., Joss P. C., Nelson L. A., 1987, ApJ, 322, 842
Ray P. S. et al., 2013, ApJ, 763, L13
Reed B. C., 1998, J. R. Astron. Soc. Canada, 92, 36
Roy J. et al., 2015, ApJ, 800, L12
Staveley-Smith L. et al., 1996, Publ. Astron. Soc. Aust., 13, 243
Stevens I. R., Rees M. J., Podsiadlowski P., 1992, MNRAS, 254, 19p
Stovall K. et al., 2014, ApJ, 791, 67
Verbiest J. P. W., Weisberg J. M., Chael A. A., Lee K. J., Lorimer D. R., 2012, ApJ, 755, 39
Wang Z., Kaplan D. L., Chakrabarty D., 2007, ApJ, 655, 261
Wolszczan A., 1997, in Soderblom D., ed., ASP Conf. Ser. Vol. 119, Planets Beyond the Solar System and the Next Generation of Space Missions. Astron. Soc. Pac., San Francisco, p. 135
Wolszczan A., Frail D. A., 1992, Nature, 355, 145
Yan Z., Shen Z.-Q., Yuan J.-P., Wang N., Rottmann H., Alef W., 2013, MNRAS, 433, 162
Yao J. M., Manchester R. N., Wang N., 2017, ApJ, 835, 29

SUPPORTING INFORMATION

Supplementary data are available at *MNRAS* online.

Please note: Oxford University Press is not responsible for the content or functionality of any supporting materials supplied by the authors. Any queries (other than missing material) should be directed to the corresponding author for the article.

This paper has been typeset from a TEX/LATEX file prepared by the author.